

Enhancement of Small Signal Stability of Multi-Machine System with DFIG using STATCOM

Ganesan U, Neslson Babu P, Santhosh Kumar T

Abstract—Integration of DFIG with the multi-machine system causes small signal stability problem i.e., oscillation in the rotor angle and speed of the synchronous machines connected in the multi-machine system due to constant variation in the generation due to uncertain nature of wind. This paper presents a control scheme based on a static synchronous compensator (STATCOM) to enhance the small signal stability of multi-machine system with DFIG by introducing positive damping in the system. A STATCOM operating on a pure voltage control mode does not provide any system damping. However, the STATCOM can contribute to system damping if it is allowed to modulate the bus voltage instead of maintaining it strictly constant. With the introduction of voltage modulating control, the STATCOM transforms the power system into a positively damped system and the eigen values of the system now lies in the left half of the s plane, and any oscillation in the rotor angle and speed will decay with time. The effectiveness of the proposed system is tested in a IEEE -9 bus system using eigen value analysis. Simulation results shows that proposed STATCOM controller is very effective to stabilize the studied system under various disturbances.

Index Terms—DFIG, STATCOM, small signal stability, eigen value, multi-machine system.

I. INTRODUCTION

DOUBLY-FED induction generator (DFIG) is, currently, the most employed wind generator due to its several merits. One of the advantages is the higher efficiency compared to a direct-drive wind power generation system with full-scale power converters since only about 20% of power flowing through power converter and the rest through stator without power electronics. Another advantage of a wind DFIG is the capability of decoupling control of active power and reactive power for better grid integration. However, by connecting stator windings directly to the power grid, a wind DFIG is extremely sensitive to grid faults. Moreover, wind energy is a kind of stochastic energy, implying that the output of Wind Farm(WF) varies in a certain range due to unstable wind characteristic. Therefore, the operating point of the power system changes from time to time when the wind power is integrated with the power system. Several published papers have discussed how to reduce the negative influences of the power grid on DFIG-based WF [1]–[5]. In [1], DFIG-based

WF connected to a power grid through a line-commutated high-voltage direct-current (HVDC) with a damping controller located at the rectifier current regulator of the HVDC link was proposed to contribute adequate damping to the WF under various wind speeds and different disturbance conditions. But this control scheme was only suitable for the systems having a long distance from WFs to grids. In [2], a variable frequency transformer (VFT) was proposed to smooth the fluctuating active power generated by the WF sent to the power grid and improve the damping of the WF. These papers, however, just considered a power grid as an infinite bus that is not a practical power system. To study the performance of a practical power system, a multi-machine power system is generally employed to replace the single-machine infinite-bus (SMIB) equivalent model. In [3], a DFIG-based wind power plant (WPP) was connected to a three-machine nine-bus system to compare voltage stability of the system at a point of common coupling when the system was with and without the WPP. The dynamic performance of DFIG-based wind turbines connected to multi-machine systems under three different configurations was presented in [4]. A new control strategy for improving fault ride-through capability of wind farms connected to a multi-machine power system was proposed in [5], while a small series dynamic braking resistor was located at the stator circuit of the DFIG along with a DC-chopper braking resistor. Especially, increase of wind-power penetration could lead to the problem of sudden disconnection of considerable amount of power generation in case of a transient fault occurred in the system, causing the system to be unstable from an otherwise harmless fault situation. In this case, a static synchronous compensator (STATCOM) is one of the good candidates for dynamic compensation of reactive power when the voltage is lower than the normal voltage range. A STATCOM can generate more reactive power than other FACTS devices like static VAR compensator (SVC). This is due to the fact that the maximum capacitive power generated by a STATCOM decreases only linearly with the bus voltage but it drops off as square of the bus voltage for an SVC. In addition, the STATCOM normally exhibits a faster response as it has no significant time delay associated with thyristor firing (in the order of 4 ms for an SVC) [6]. In [7], a STATCOM was connected at the point of common coupling (PCC) to maintain stable voltage and to improve the power quality by protecting DFIG-based wind farm connected to a weak grid from going offline during and after disturbances. As proposed in [8], a new control strategy using a full-power wind permanent-magnet generator (PMG) with a STATCOM to provide reactive power compensation can be used to improve stability of transient voltage. In [9], performance of a PMG-based wind energy system employing a dynamic

Manuscript received November 06, 2013.

Ganesan U, Department of Electrical and Electronics Engineering, Valliammai Engineering College, Chennai, India, +91 9789814197.

Nelson Babu P, Department of Electrical and Electronics Engineering, Valliammai Engineering College, Chennai, India, +91 9444034484.

Santhosh Kumar T, Department of Electrical and Electronics Engineering, Valliammai Engineering College, Chennai, India, +91 9884408823.

voltage regulator (DVR) was compared to one of the system employing a STATCOM. It is recommended to use a STATCOM in systems with large loads where reactive power consumption from the grid could cause serious effects on connected loads. For the purpose of improving the damping of the studied power system for grid integration of an WF, this paper proposes a STATCOM connected to the interconnected bus of a DFIG-based WF fed to a three-machine nine-bus system for compensating reactive power and maintaining the voltage at the connected bus. The main contribution of this study is the STATCOM controller considered as a new damping controller which is designed to damp out oscillations of the studied system. This paper is organized as below. Mathematical model of the studied DFIG-based WF fed to a three-machine nine-bus system using a STATCOM are introduced in Section II. The damping actions of proposed STATCOM controller using voltage modulation by feedback of auxiliary signals are depicted in Section III. System state matrix formation is discussed in section IV. Simulation results using eigen value analysis under various operation points are described in Sections V. Finally some important conclusions of this paper are drawn in Section VI.

II. MULTI-MACHINE SYSTEM AND DFIG MODELS

A. Three machine Nine-Bus System

The state space model of the multi-machine system is given by [10]

$$\begin{bmatrix} \Delta \delta_i \\ \Delta \omega_i \\ \Delta E'_{qi} \\ \Delta E'_{di} \\ \Delta E'_{fdi} \\ \Delta V_{Ri} \\ \Delta R_{Fi} \end{bmatrix} = \begin{bmatrix} 0 & 1 & 0 & 0 & 0 & 0 & 0 \\ 0 & \frac{-D_i}{M_i} & \frac{-I_{qi} \omega}{M_i} & \frac{-I_{dio}}{M_i} & 0 & 0 & 0 \\ 0 & 0 & \frac{-1}{T'_{doi}} & 0 & \frac{1}{T'_{doi}} & 0 & 0 \\ 0 & 0 & 0 & \frac{-1}{T_{qoi}} & 0 & 0 & 0 \\ 0 & 0 & 0 & 0 & f_i(E_{fDio}) & \frac{1}{T_{Ei}} & 0 \\ 0 & 0 & 0 & 0 & \frac{-K_{Ai} T_{Fi}}{T_{Ai} T_{Fi}} & \frac{1}{T_{Ai}} & \frac{K_{Ai}}{T_{Ai}} \\ 0 & 0 & 0 & 0 & \frac{K_{Fi}}{T_{Fi}} & 0 & \frac{-1}{T_{Fi}} \end{bmatrix} \begin{bmatrix} \Delta \delta_i \\ \Delta \omega_i \\ \Delta E'_{qi} \\ \Delta E'_{di} \\ \Delta E'_{fdi} \\ \Delta V_{Ri} \\ \Delta R_{Fi} \end{bmatrix} \quad (1)$$

Here the synchronous machines are modelling are done using two axis model and IEEE type 1 exciter is used. Where δ_i is the rotor angle of ith machine, ω_i is speed of the ith machine E'_{qi} is the quadrature axis voltage of ith machine, E'_{di} is the direct axis voltage of ith machine, E'_{fdi} is the field voltage of ith machine, V_{Ri} reference voltage of ith machine, D_i is the damping constant of ith machine, M_i is the inertia constant of ith machine, T'_{doi} is the transient open circuit time constant, T_{qoi} is the transient open circuit time constant, I_{dio} is the direct axis current of ith machine, I_{qio} is the quadrature axis current of ith machine and K_{Ai} , T_{Fi} exciter constant of ith machine.

B. Mass Spring Damper Model of Wind Turbine

The state space model of two-inertia reduced order wind turbine is given by [11]

$$p \begin{bmatrix} \omega_H \\ \omega_g \\ \theta_{Hg} \end{bmatrix} = \begin{bmatrix} \frac{-D_{Hg}}{2H_H} & 0 & \frac{-K_{Hg}}{2H_H} \\ 0 & \frac{D_{Hg}}{2H_g} & \frac{K_{Hg}}{2H_g} \\ \omega_b & -\omega_b & 0 \end{bmatrix} \begin{bmatrix} \omega_H \\ \omega_g \\ \theta_{Hg} \end{bmatrix} \quad (2)$$

where H_H and H_g (ω_H and ω_r) are, respectively, the inertias (angular speeds) of hub and IG, D_{Hg} , K_{Hg} , and θ_{Hg} are, respectively, the mechanical damping coefficient, spring constant, and rotor angle difference between hub and IG, T_m is the mechanical input torque, T_e is the electromagnetic torque of IG that can be expressed by $T_e = X_m(i_{dr}i_{qs} - i_{qr}i_{ds})$, and p is the differential operator with respect to time t .

C. DFIG Model

The per unit q and d axis voltage-current equations of an induction generator can be referred to and they can be used for electrical parts of DFIG. The state space model of the DFIG is given by[11]

$$p \begin{bmatrix} i_{ds} \\ i_{qs} \\ i_{dr} \\ i_{qr} \end{bmatrix} = K \begin{bmatrix} -r_s x_r & \omega_e x_s x_r - (\omega_e - \omega_g) x_m^2 & -r_r x_m & -\omega_g x_m x_r \\ -\omega_e x_s x_r + (\omega_e - \omega_g) x_m^2 & -r_s x_r & \omega_g x_m x_r & -r_r x_m \\ -r_s x_m & \omega_g x_s x_m & -r_r x_s & -\omega_e x_m^2 + (\omega_e - \omega_g) x_s x_r \\ -\omega_g x_s x_m & -r_s x_m & -\omega_e x_m^2 + (\omega_e - \omega_g) x_s x_r & -r_r x_s \end{bmatrix} \begin{bmatrix} i_{ds} \\ i_{qs} \\ i_{dr} \\ i_{qr} \end{bmatrix}$$

$$\text{Where } K = \frac{\omega_b}{x_s x_r - x_m^2} \quad (3)$$

where X_m is the mutual reactance between the stator and rotor, and $X_{ss} = X_l + X_m$ and $X_{rr} = X_l + X_m$ (X_l and X_l) are, respectively, the self (leakage) reactances of the stator and the rotor windings.

D. STATCOM Model

Two axis model using pu q-d axis equations are used for modeling STATCOM. The state space model of the STATCOM is given by[15]

$$p \begin{bmatrix} v_{qsta} \\ v_{dsta} \\ i_{qsta} \\ i_{dsta} \\ v_{DC} \end{bmatrix} = \begin{bmatrix} 0 & 0 & \frac{k_m^2 \omega_b \cos^2(\theta + \alpha)}{C_m} & \frac{k_m^2 \omega_b \cos(\theta + \alpha) \sin(\theta + \alpha)}{C_m} & \frac{-k_m \omega_b \cos(\theta + \alpha)}{C_m R_m} \\ 0 & 0 & \frac{k_m^2 \omega_b \cos(\theta + \alpha) \sin(\theta + \alpha)}{C_m} & \frac{k_m^2 \omega_b \sin^2(\theta + \alpha)}{C_m} & \frac{-k_m \omega_b \sin(\theta + \alpha)}{C_m R_m} \\ \frac{-\omega_b}{X_{sta}} & 0 & \frac{-\omega_b R_{sta}}{X_{sta}} & -\omega_e \omega_b & 0 \\ 0 & \frac{-\omega_b}{X_{sta}} & -\omega_e \omega_b & \frac{-\omega_b R_{sta}}{X_{sta}} & 0 \\ 0 & 0 & \frac{k_m \omega_b \cos(\theta + \alpha)}{C_m} & \frac{k_m \omega_b \sin(\theta + \alpha)}{C_m} & \frac{-\omega_b}{C_m R_m} \end{bmatrix} \begin{bmatrix} v_{qsta} \\ v_{dsta} \\ i_{qsta} \\ i_{dsta} \\ v_{DC} \end{bmatrix} \quad (4)$$

Where Θ is the phase angle of bus at which STATCOM is placed, α_{sta} is the phase angle of STATCOM (varies V_{dcsta}), k_m is the modulation index (varies V_{sta}), V_{qsta} is the q axis voltage of STATCOM, V_{dsta} is the d axis voltage of STATCOM, I_{qsta} is the q axis current of STATCOM, I_{dsta} is the d axis current of STATCOM, V_{dcsta} is the dc voltage of the STATCOM energy storage system.

III. DAMPING CONTROLLER ACTION OF THE STATCOM

In this section the damping controller action of the STATCOM is explained. Consider a two bus two machine system as shown in the Fig. 1.



Fig. 1 A two bus two machine system

Let $V_1 = |V_1|\sin(\omega t)$ and $V_2 = |V_2|\sin(\omega t + \delta)$.

The swing equation of the system can be written as

$$M \frac{d^2\delta}{dt^2} = P_M - P_E \quad (6)$$

where M = angular momentum of the synchronous generator

δ = the generator rotor angle.

For small signal analysis, (6) is linearized as

$$M \frac{d^2\Delta\delta}{dt^2} = \Delta P_M - \Delta P_E \quad (7)$$

The mechanical input power is assumed to be constant during the time of analysis; hence $\Delta P_M = 0$. The linearized swing equation then becomes

$$M \frac{d^2\Delta\delta}{dt^2} = -\Delta P_E \quad (8)$$

The electrical power P_E transmitted across the line, is given by

$$P_E = \frac{V_1 V_2}{X} \sin \delta \quad (9)$$

An incremental change in electrical power is obtained by linearizing (9) as

$$\Delta P_E = \frac{\partial P_E}{\partial V_1} \Delta V_1 + \frac{\partial P_E}{\partial V_2} \Delta V_2 + \frac{\partial P_E}{\partial \delta} \Delta \delta \quad (10)$$

It is further assumed that the sending end voltage is constant; thus $\Delta V_1 = 0$. Substituting ΔP_E from (10) in (8) results in

$$M \frac{d^2(\Delta\delta)}{dt^2} + \frac{\partial P_E}{\partial V_2} \Delta V_2 + \frac{\partial P_E}{\partial \delta} \Delta \delta = 0 \quad (11)$$

(11) describes the small signal dynamic behavior of the system, in which the effect of the STATCOM is represented by the middle term. If the STATCOM is operated to maintain the voltage V_2 strictly constant as is done for voltage control, ΔV_2 becomes zero, in which case (11) reduces to

$$M \frac{d^2(\Delta\delta)}{dt^2} + \frac{\partial P_E}{\partial \delta} \Delta \delta = 0 \quad (12)$$

The characteristics equation corresponding to (12) is

$$s^2 + \frac{1}{M} \frac{\partial P_E}{\partial \delta} = 0 \quad (13)$$

The roots of (13) lie on the imaginary axis that result in undamped oscillation in the rotor angle δ with a frequency of

$$\omega_n = \sqrt{\frac{1}{M} \frac{\partial P_E}{\partial \delta}} \quad (14)$$

Where $\frac{\partial P_E}{\partial \delta}$ is the synchronizing power coefficient. It is clearly evident that STATCOM operating on pure voltage control mode is unable to provide any system damping. However the STATCOM can contribute to system damping if it is allowed to modulate the receiving end voltage V_2 instead of maintaining it strictly constant. Specifically, the midpoint voltage can be modulated as a function of $\frac{d(\Delta\delta)}{dt}$, that is

$$\Delta V_2 = K \frac{d(\Delta\delta)}{dt} \quad (15)$$

Where K is a constant. Substituting (15) in (11) results in modified incremental swing equation

$$M \frac{d^2(\Delta\delta)}{dt^2} + \frac{\partial P_E}{\partial V_2} \cdot K \cdot \frac{d(\Delta\delta)}{dt} + \frac{\partial P_E}{\partial \delta} \Delta \delta = 0 \quad (16)$$

The corresponding characteristics equation is

$$s^2 + 2\xi s + \omega_n^2 = 0 \quad (17)$$

Where

$$2\xi = \frac{K}{M} \frac{\partial P_E}{\partial V_2} \quad (18)$$

With the introduction of the voltage modulating control, the STATCOM transforms the power system into a positively damped system. From (17), it is seen that the roots now lie on the left half of the s plane, and any oscillations in the rotor angle will decay with time. Such an additional control feature is termed auxiliary control, supplementary control, or power swing damping control. One effective signal for improving system damping, as seen in this analysis is the variation in bus frequency f , for it relates to the rotor angle oscillations:

$$\frac{d(\Delta\delta)}{dt} = \Delta f \quad (19)$$

An intuitive insight into the mechanism of auxiliary control is as follows: at any instant if $\frac{d(\Delta\delta)}{dt}$ is positive, it is implied that the rotor is tending to accelerate from the buildup of the kinetic energy within it. This buildup can be alleviated by adjusting the STATCOM control so that the generator electrical power output is increased during that particular time interval, which requires an increase in the STATCOM terminal voltage. On the other hand if $\frac{d(\Delta\delta)}{dt}$ is negative, indicating rotor deceleration, the electrical power output of the generator must be decreased by reducing the STATCOM terminal voltage through damping controller action. The auxiliary controllers of the STATCOM greatly enhance the flexibility and performance capability of the STATCOM without requiring any increase in the rating.

IV. SYSTEM STATE MATRIX FORMATION

The nonlinear system equations developed in the previous section are linearized around a selected nominal operating point to acquire a set of linearized system equations in matrix form of

$$pX = AX + BU + D$$

$$Y = CX + DU \tag{20}$$

Where X is the state vector, Y is the output vector, U is the external or compensated input vector, W is the disturbance input vector while A .B,C and D are all constant matrices of appropriate dimensions. The state vector can be partitioned into three substate vectors as $X = [X_{SGs}, X_{WT-DFIG}, X_{STATCOM}]^T$, where X_{SGs} , $X_{WT-DFIG}$ and $X_{STATCOM}$ are referred to the system state vectors of the three SGs, the DFIG-based OWF, and the STATCOM, respectively. Here A is the final system matrix whose eigen value need to be calculated for small signal stability analysis.

V.SIMULATION RESULTS

The simulation of the proposed system is carried out using Power System Analysis Toolbox (PSAT) software on a IEEE-9 bus system. Fig. 2 and Fig. 3 shows the simulation of the system without and with STATCOM respectively.

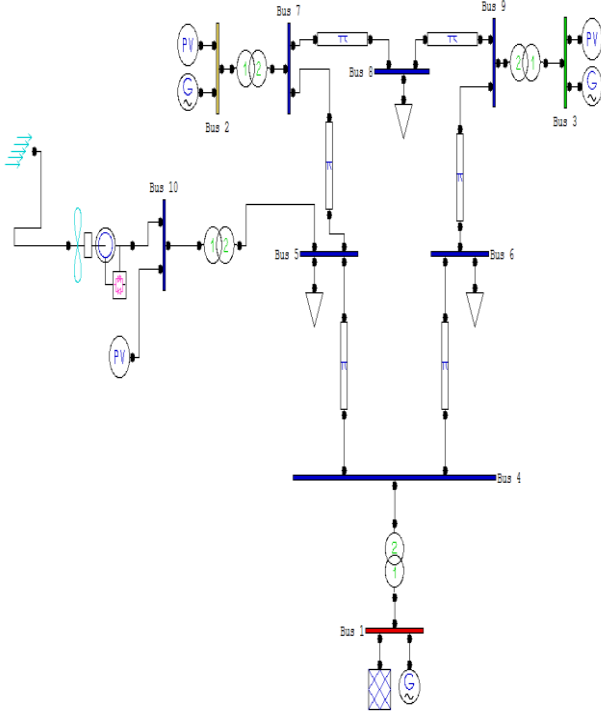


Fig. 2 IEEE-9 bus system with DFIG WF connected at bus 5

The IEEE-9 bus system which was described in detail [12] is used to demonstrate the small signal stability analysis of the power system with large scale wind turbines. The test system shown in Fig. 2 has three generators, providing both active and reactive power at Buses 1 and 2, and 3. Each machine is so generally equipped with an Automatic Voltage Regulator (AVR). The generators are modelled using subtransient

models, and loads are modelled as constant power loads (PQ load) in PSAT. A 100 MVA DFIG wind farm composed of 20 individual DFIGs are integrated to the system at bus 5 through step up transformer as shown in Fig. 2.A comparative study of eigen values before and after the placement of STATCOM at bus 5 is done . Table I shows the eigenvalue of sytem with only DFIG WF connected at bus 5 for a base wind speed of 15 m/s. It can be observed that the eigen values associated with the rotor angle and speed of the three synchronous generator lie on the imaginary axis of the s plane and is oscillatory stable. Table II shows the eigen value of the same system after a sudden increase in the wind speed to 17 m/s. It can be observed that the eigen values associated with the rotor angle and speed of three synchronous machine crosses the imaginary axis and settles on the right half of the s plane making the three synchronous machine unstable. It causes oscillation in the rotor angle and speed. And also fluctuation in the real power that is transferred . If these oscillations are allowed to prolong then it results in the generator trip and complete loss of stability. Hence it can be concluded that integration of wind energy source is a source of disturbance unless some compensating technique is adopted. Table III shows the eigen value of the system after connecting a STATCOM at the bus 5 where the DFIG WF is integrated for base wind speed. It can be observed that the the eigen values associated with the rotor angle and speed of the three synchronous generator now lies in the left half of the s planes making these modes viz., rotor angle and speed stable.

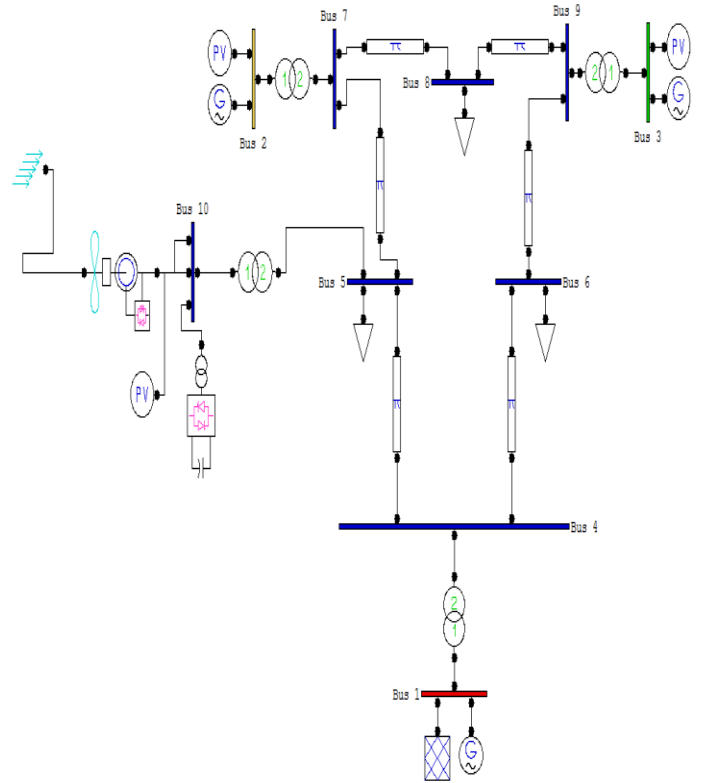


Fig. 3 IEEE- 9 bus system with DFIG WF and STATCOM connected at bus 5

This is due to the modulation of the bus voltage by STACOM through feedback of rotor angle deviation signal, instead of holding the voltage constant during the disturbance condition. We can also observe that the eigen value associated with the STATCOM (current injected) is also lies on left half of the s plane.

TABLE I
EIGEN VALUE OF THE STUDIED SYSTEM UNDER BASE WIND SPEED OF 15 M/S

Eigen Value	Most associated states	Real Part	Imaginary Part
Eig As# 1	omega_Syn_2, delta_Syn_2	0	12.1948
Eig As# 2	omega_Syn_2, delta_Syn_2	0	-12.1948
Eig As# 3	delta_Syn_1, omega_Syn_1	0	8.0337
Eig As# 4	delta_Syn_1, omega_Syn_1	0	-8.0337
Eig As# 5	omega_Syn_3	0	0
Eig As# 6	delta_Syn_3	0	0
Eig As# 7	vw_Wind_1	-0.25	0
Eig As# 8	omega_m_Dfig_1	-1	0
Eig As# 9	theta_p_Dfig_1	-2.5	0
Eig As# 10	idr_Dfig_1	-1	0
Eig As# 11	iqr_Dfig_1	-100	0

TABLE II
EIGEN VALUE OF THE STUDIED SYSTEM AFTER INCREASING WIND SPEED TO 17 m/s

Eigen Value	Most associated states	Real Part	Imaginary Part
Eig As# 1	omega_Syn_2, delta_Syn_2	0.39825	0.91728
Eig As# 2	omega_Syn_2, delta_Syn_2	0.39825	-0.91728
Eig As# 3	delta_Syn_1, omega_Syn_1	0.0042	0.99999
Eig As# 4	delta_Syn_1, omega_Syn_1	0.0042	-0.99999
Eig As# 5	omega_Syn_3	-1	0
Eig As# 6	delta_Syn_3	-1	0
Eig As# 7	vw_Wind_1	-0.93939	0
Eig As# 8	omega_m_Dfig_1	-0.77778	0
Eig As# 9	theta_p_Dfig_1	-0.52381	0
Eig As# 10	idr_Dfig_1	-0.77778	0
Eig As# 11	qr_Dfig_1	0.85185	0

Table IV shows the eigen value for the same case of the base wind speed with increased STATCOM gain. Again it can be observed that the eigen values associated with rotor angle and speed of the three synchronous generator lies on the left half of the s plane. The proposed STATCOM controller can supply better damping characteristics to quickly damp out the inherent oscillation of the studied system than the studied system without STATCOM controller.

TABLE III

EIGEN VALUES OF THE SYSTEM AFTER INTEGRATION OF STATCOM AT BUS 5

Eigen Value	Most associated states	Real Part	Imaginary Part
Eig As# 1	ist_Statcom_1	-314.7859	0
Eig As# 2	omega_Syn_2, delta_Syn_2	-1e-05	12.1931
Eig As# 3	omega_Syn_2, delta_Syn_2	-1e-05	-12.1931
Eig As# 4	delta_Syn_1, omega_Syn_1	-0.00199	8.0495
Eig As# 5	delta_Syn_1, omega_Syn_1	-0.00199	-8.0495
Eig As# 6	omega_Syn_3, delta_Syn_3	-0.05652	1.2985
Eig As# 7	delta_Syn_3, omega_Syn_3	-0.05652	-1.2985
Eig As# 8	omega_m_Dfig_1	-0.5912	0
Eig As# 9	idr_Dfig_1	-1.0553	0
Eig As# 10	vw_Wind_1	-0.25	0
Eig As# 11	theta_p_Dfig_1	-2.5	0
Eig As# 12	iqr_Dfig_1	-100	0

TABLE IV

EIGEN VALUES OF THE SYSTEM WITH INCREASED STATCOM GAIN

Eigen Value	Most associated states	Real Part	Imaginary Part
Eig As# 1	ist_Statcom_1	-415.7691	0
Eig As# 2	omega_Syn_2, delta_Syn_2	-1e-05	12.1931
Eig As# 3	omega_Syn_2, delta_Syn_2	-1e-05	-12.1931
Eig As# 4	delta_Syn_1, omega_Syn_1	-0.00146	8.0501
Eig As# 5	delta_Syn_1, omega_Syn_1	-0.00146	-8.0501
Eig As# 6	omega_Syn_3, delta_Syn_3	-0.05652	1.2986
Eig As# 7	delta_Syn_3, omega_Syn_3	-0.05652	-1.2986
Eig As# 8	omega_m_Dfig_1	-0.5912	0
Eig As# 9	idr_Dfig_1	-1.0419	0
Eig As# 10	vw_Wind_1	-0.25	0
Eig As# 11	theta_p_Dfig_1	-2.5	0
Eig As# 12	iqr_Dfig_1	-100	0

VI. CONCLUSION

This paper has presented the stability enhancement of a DFIG-based WF fed to a multi-machine system using a STATCOM. The STATCOM is proposed and is connected to the bus of the WF to the multi-machine system. To introduce adequate damping in power system, a damping controller for the STATCOM has been designed by voltage modulation through feedback of rotor can be concluded from the simulation results that the proposed STATCOM joined with the designed damping controller best damping characteristics to improve the performance of the DFIG-based WF fed to the studied multi-machine system under different operating conditions. angle signal. Eigen value analysis under various wind speed operating conditions have been carried to show the effectiveness of the designed damping controller for the STATCOM. It can be concluded from the simulation results that the proposed STATCOM joined with the designed damping controller best damping characteristics to improve the performance of the DFIG-based WF fed to the studied multi-machine system under different operating conditions.

REFERENCES

- [1] L. Wang and K.-H. Wang, "Dynamic stability analysis of a DFIG-based offshore wind farm connected to a power grid through an HVDC link," *IEEE Trans. Power Syst.*, vol. 26, no. 3, pp. 1501–1510, Aug. 2010.
- [2] L. Wang and L.-Y. Chen, "Reduction of power fluctuations of a large-scale grid-connected offshore wind farm using a variable frequency transformer," *IEEE Trans. Sustain. Energy*, vol. 2, no. 3, pp. 226–234, Apr. 2011.
- [3] E. Muljadi, T. B. Nguyen, and M.A. Pai, "Impact of wind power plants on voltage and transient stability of power systems," in *Proc. IEEE Energy 2030 Conf.*, Nov. 2008, pp. 1–7.
- [4] O. Anaya-Lara, A. Arulampalam, G. Bathurst, F. M. Hughes, and N. Jenkins, "Transient analysis of DFIG wind turbines in multi-machine networks," in *Proc. 18th Int. Conf. Exhib. Electricity Distribution CIRED*, Jun. 2005, pp. 1–5.
- [5] K. E. Okedu, S.M. Muyeen, R. Takahashi, and J. Tamura, "Improvement of fault ride through capability of wind farms using DFIG considering SDBR," in *Proc. 14th Eur. Conf. Power Electronics and Applications*, Sep. 2011, pp. 1–10.
- [6] N. G. Hingorani and L. Gyugyi, *Understanding FACTS; Concepts and Technology of Flexible AC Transmission Systems*. New York, NY, USA: IEEE Press, 2000.
- [7] B. Pokharel and W. Gao, "Mitigation of disturbances in DFIG-based wind farm connected to weak distribution system using STATCOM," in *Proc. North American Power Symp. (NAPS)*, Sep. 26–28, 2010, pp. 1–7.
- [8] G. Cai, C. Liu, Q. Sun, D. Yang, and P. Li, "A new control strategy to improve voltage stability of the power system containing large-scale wind power plants," in *Proc. 4th Int. Conf. Electric Utility Deregulation and Restructuring and Power Technologies (DRPT)*, Jul. 2011, pp. 1276–1281.
- [9] M.N. Eskander and S. I. Amer, "Mitigation of voltage dips and swells in grid-connected wind energy conversion systems," in *Proc. ICCASSICE*, Aug. 2009, pp. 885–890.
- [10] P. W. Sauer and M. A. Pai, *Power System Dynamics and Stability*. Englewood Cliffs, NJ, USA: Prentice Hall, 1998.
- [11] L. Wang, S.-S. Chen, W.-J. Lee, and Z. Chen, "Dynamic stability enhancement and power flow control of a hybrid wind and marine-current farm using SMES," *IEEE Trans. Energy Convers.*, vol. 24, no. 3, pp. 626–639, Sep. 2009.
- [12] M. N. Uddin and R. S. Rebeiro, "Improved dynamic and steady state performance of a hybrid speed controller based IPMSM drive," in *Proc. IEEE Industry Applications Society Annual Meeting (IAS)*, Oct. 9–13, 2011, pp. 1–8.
- [13] S. M. Muyeen, M. H. Ali, R. Takahashi, T. Murata, J. Tamura, Y. Tomaki, A. Sakahara, and E. Sasano, "Transient stability analysis of wind generator system with the consideration of multi-mass shaft model," in *Proc. Int. Conf. Power Electronics and Drives Systems*, Jan. 16–18, 2006, vol. 1, pp. 511–516.
- [14] F. Wu, X.-P. Zhang, K. Godfrey, and P. Ju, "Small signal stability analysis and optimal control of a wind turbine with doubly fed induction generator," *IET Gen., Transm., Distrib.*, vol. 1, no. 5, pp. 751–760, Sep. 2007.
- [15] L. Wang and C.-T. Hsiung, "Dynamic stability improvement of an integrated grid-connected offshore wind farm and marine-current farm using a STATCOM," *IEEE Trans. Power Syst.*, vol. 26, no. 2, pp. 690–698, May 2011.